Proceedings of the 9th U.S. National and 10th Canadian Conference on Earthquake Engineering
Compte Rendu de la 9ième Conférence Nationale Américaine et
10ième Conférence Canadienne de Génie Parasismique
July 25-29, 2010, Toronto, Ontario, Canada • Paper No 1040

EVALUATION OF THE BENDING BEHAVIOR OF HOLLOW STRUCTURAL SECTION (HSS) MEMBERS FOR SEISMIC APPLICATIONS

Matthew Fadden[1] and Jason McCormick[2]

ABSTRACT

Hollow structural sections (HSS) are highly efficient when resisting torsion, compression, and bending. However, their use typically has been limited to columns rather than beams for steel moment frame systems constructed in areas of high seismicity. Current design standards for seismic moment connections require the majority of the inelastic behavior to occur in the beam member (i.e. strong column-weak beam design). In order to increase the use of HSS members in seismic moment frame systems, it is necessary to determine their ability to form stable plastic hinges under cyclic deformations. To address this requirement, an experimental study is undertaken to examine the bending behavior of HSS beam members under large cyclic deformations up to drift levels as high as 0.7 rad. Stock square and rectangular HSS beam members ranging in size from HSS203.2x101.6x9.5 mm to HSS203.2x203.2x9.5 mm are considered with plastic moments ranging from 87.8 kN-m (777 kip-in) to 152.7 kN-m (1352 kip-in). Stable plastic hinge behavior is obtained when the width-to-thickness ratio remains below or near the seismically compact limit of 16.1. However, when the width-to-thickness ratio is above 22, degradation of up to 46% of the maximum moment during later cycles is observed. The results clearly show that lower width-to-thickness ratios provide more stable post yield behavior which suggests that the use of HSS beam members in moment frames is viable.

Introduction

Steel moment frames are a widely used means of providing lateral load resistance in areas of high seismicity. This is particularly true when considering low to mid-rise frames where rigid frame action provides lateral load resistance through the development of bending moments and shear forces in the frame members and joints. As a result, moment frames are often viewed as highly ductile systems allowing for a significant reduction in the lateral design forces. However, significant damage was sustained by steel moment frames during both the 1994 Northridge earthquake and 1995 Hyogoken-Nanbu (Kobe) earthquake due to brittle failure at the beam-

[1]Graduate Research Assistant, Dept. of Civil & Environmental Engineering, University of Michigan, Ann Arbor, MI 48109-2125
[2]Assistant Professor, Dept. of Civil & Environmental Engineering, University of Michigan, Ann Arbor, MI 48105-2125

column connections. This damage caused questions in regards to the ductility of steel moment frame systems and forced the need to more closely identify the reason for the observed brittle failure in the moment connections (Nakashima et al. 2000). In the United States, this need was addressed through the joint SAC steel project which led to further improvements in the design of steel moment frame systems and a better understanding of the underlying mechanisms associated with moment frame connections under large cyclic loads (FEMA 2000). The majority of this work focused on wide flange member connections and did not explore the use of other types of members, such as hollow structural sections (HSS).

In comparison to other conventional sections, HSS are highly efficient in terms of resisting compression, bending, and torsion. The efficiency of these sections suggests the possibility of higher ductility and hysteretic energy dissipation capacity when undergoing large inelastic cycling associated with a seismic event. Until now, most of the attention focused on HSS connections has been on axial loaded and truss-type connections or concrete filled tube (CFT) to wide flange moment connections where the majority of the studies of onshore tubular structures have been conducted outside the United States (Packer 2000; Hajjar 2000; Kurbane 2002; Nishiyama and Morino 2004). Since current performance-based design requires proportioning the beam and column member such that strong column-weak beam behavior is obtained, it is imperative that the bending behavior of HSS members be better understood in order to utilize them as both beams and columns in seismic moment connections for low to mid-rise frames.

Few previous studies have looked at the bending behavior of HSS members under a variety of loadings. Most studies of HSS-to-HSS moment connections were completed back in the 1970's and focused on Vierendeel truss connections. A study by Korol et al. (1977) focused on five types of connections based on the importance of the beam width to column wall thickness ratio. Other studies showed that the predominant failure modes were column face plastification, effective beam width failure, and column sidewall crippling (Packer and Henderson, 1997). These studies mainly focused on monotonic loadings. Studies which have considered cyclic loading were focused on HSS columns which have larger axial loads than those expected in HSS beam members (Kurata et al 2005; Nakashima and Liu 2005; Wang et al. 2008). Only a few studies have looked into the behavior of HSS-to-HSS moment connections under seismic type loads where the results suggest the possibility of further development of such connections (Wheeler et al 1998; Wheeler et al 2000; Kumar and Rao 2006; Rao and Kumar 2006). However, there continues to be a need to better understand the behavior of HSS under cyclic bending to utilize them fully in tubular moment frame structures.

In order to address the lack of knowledge with respect to the bending behavior of HSS members, an experimental study was carried out to investigate the ability of HSS beams to form viable plastic hinges under large cyclic loads. Square and rectangular HSS beam members ranging in size from HSS203.2x101.6x9.5 mm (HSS8x4x3/8 in.) to HSS203.2x203.2x9.5 mm (HSS8x8x3/8 in.) were considered. The study provided important insight into limiting factors, such as the width-to-thickness ratio and depth-to-thickness ratio, for the use of HSS beams in low to mid-rise moment frames. The failure mode of each specimen also was observed and compared. The backbone curves associated with the normalized moment-rotation behavior provided a further means of comparing the test specimens' ability to form stable plastic hinges.

Cyclic Testing of HSS Beam Members

A systematic experimental study was undertaken to examine the behavior of full-scale HSS beams under large cyclic deformations. The ability of an HSS beam to develop appropriate plastic hinge behavior consistent with strong column-weak beam moment frame design is imperative for expanding the use of HSS members to seismic moment frame systems.

Test Specimens

One square and three rectangular HSS were chosen for this portion of an ongoing study exploring the influence of the wall thickness, width-to-thickness ratio, and depth-to-thickness ratio on the moment-rotation behavior of HSS. Table 1 lists the four HSS along with various properties associated with each section. Standard U.S. cold formed sections were selected with a minimum tensile yield strength, F_y, of 317×10^3 kN/m^2 (46 ksi). This value of F_y was used to calculate the theoretical plastic moment strength ($M_p = Z_x F_y$) throughout the paper. These sections allowed for an investigation of the compactness requirements associated with HSS for seismic moment frames provided by the American Institute of Steel Construction Seismic Provisions for Structural Steel Buildings (AISC 2006). Current requirements state that the width-to-thickness and depth-to-thickness ratios for HSS elements must be less than 16.1. The selected sections provided width-to-thickness ratios above, below, and near this value. The depth-to-thickness ratio was above 16.1 for all specimens due to the need to consider larger depths for beam members. The chosen wall thicknesses, 6.35 mm (0.25 in.) and 9.53 mm (0.375 in.), are typical of those that may be used in low to mid-rise moment frames. The plastic moment capacity for these sections ranged between 87.8 kN-m (777 kip-in) and 152.7 kN-m (1352 kip-in).

Table 1. HSS properties along with theoretical plastic moment values and plastic hinge lengths

Member (mm x mm x mm)	**Area** A_g (mm^2)	**Wall Thickness** t (mm)	**Width to Thickness Ratio** b/t	**Depth to Thickness Ratio** h/t	**Plastic Sec. Mod.** Z_x (cm^3)	**Plastic Moment** M_p (kN-m)	**Hinge Length** L_p (mm)
HSS203.2x101.6x9.5	4889	8.86	8.46	19.9	308	97.7	333
HSS203.2x152.4x6.4	3980	5.91	22.8	31.3	277	87.8	244
HSS203.2x152.4x9.5	5786	8.86	14.2	19.9	395	125.3	272
HSS203.2x203.2x9.5	6708	8.86	19.9	19.9	482	152.7	233

Experimental Setup

The experimental tests were conducted assuming a fully rigid connection and essentially ignoring panel zone and column deformations to isolate the plastic hinge behavior. This was accomplished by cantilevering the HSS beam and applying a horizontal displacement to the free end. In order to provide a rigid and reusable connection at the fixed end, two stiffened angle members sandwiched the compression and tension flange of the HSS member. The connection was further stiffened and welded to ensure that the inelastic deformation occurred in the plastic hinge region. Fig. 1 shows a schematic and photo of the test setup where a preexisting load frame was used to apply the horizontal displacement. The HSS beam was set vertically with the fixed end connected to the bottom beam of the load frame. A pin connection transferred the load to the HSS member. The pin passed through a slotted hole in the HSS to avoid the application of vertical load, which allowed for a better understanding of the behavior of HSS beams under pure bending. A 445 kN (100 kip) hydraulic actuator applied the required displacement at a quasi-static loading rate. Since the load frame allowed for a horizontal displacement of 127 mm (5 in.) and the specimen length was approximately 1535 mm (60.5 in.), a maximum beam rotation of 0.08 rad was considered.

An optical position sensing system provided the displacement measurements. The optical markers were attached to the web of the HSS beam in a 76 mm (3 in.) by 76 mm (3 in.) grid within the plastic hinge region. Strain gages were placed on the flanges of the HSS members at distances of 76 mm (3 in.), 229 mm (9 in.), 457 mm (18 in.) and 914 mm (36 in.) from the fixed connection. A load cell attached to the actuator measured the horizontal load while the optical position sensing system measured the horizontal displacement of the pin. In order to better see the initiation of yielding and buckling in the plastic hinge region, the flanges and web opposite that containing the optical markers were whitewashed.

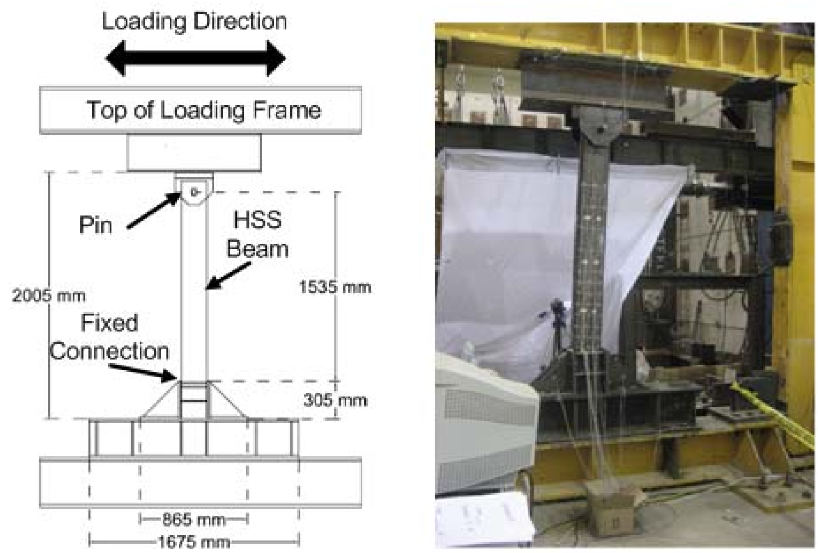

Figure 1. Schematic and photograph of the test setup and instrumentation.

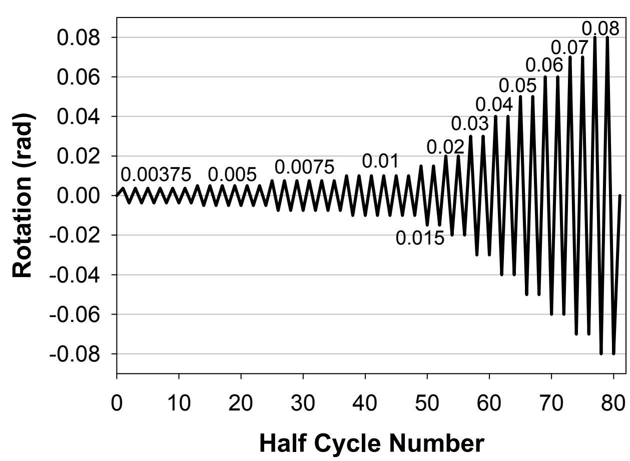

Figure 2. Loading protocol used for the experimental study in terms of beam rotation.

Loading Protocol

All tests were run in displacement control. The loading protocol can be seen in Fig. 2 and was consistent with the protocol required by the AISC Seismic Provisions (2006) for the qualification of beam-to-column moment connections. The beam rotation was defined as the horizontal displacement of the top of the beam divided by the height of the loading pin from the fixed connection. The loading protocol allowed for consideration of the cyclic behavior of HSS beams in bending and provided insight into the failure of such sections under large deformation levels where data was limited. However, due to the test configuration, the beam experienced some rigid body rotation resulting in smaller rotation levels than those specified by the loading protocol. As a result, the full rotation of 0.08 rad was not reached, but all specimens were cycled to rotation levels greater than 0.045 rad. For all of the data presented, the rigid rotation, which was measured using the optical system, was subtracted from the measured rotation based on the pin displacement to give the actual deformation experienced by the member.

HSS Beam Behavior and Observations

All four of the HSS members tested maintained some amount of load carrying capacity throughout the full loading protocol. The behavior of each specimen was highly dependent on the variation in the width-to-thickness ratios. Both the HSS203.2x101.6x9.5 and HSS203.2x152.4x9.5 (HSS8x6x3/8 in.) had compression flanges whose slenderness were below the limiting value, 16.1, specified by AISC. As a result, it was expected that yielding, rather than local buckling, would control the behavior of these specimens. The HSS203.2x101.6x9.5 specimen clearly demonstrated this with no visible signs of buckling even after cycling to maximum rotations of 0.06 rad. Fig. 3(a) shows a photograph of the HSS203.2x101.6x9.5 specimen upon completion of the test were it was evident that no local buckling of the flange occurred. Even though the depth-to-thickness ratio for this specimen was greater than the limiting slenderness value, no buckling of the web was observed as well. Likewise, the HSS203.2x152.4x9.5 specimen demonstrated very stable behavior. Since the width-to-thickness ratio, 14.2, for this specimen was much closer to the limiting value, minor buckling of the flange was observed. This buckling initiated with rotations of 0.04 rad. This was evident in Fig. 3(b) where yield lines are visible along with a slight outward deformation of the flange wall. The flange buckling remained minor up through the maximum cycles of 0.055 rad and web yielding continued to propagate toward its center as seen in Fig. 3(c).

The width-to-thickness ratio of the HSS203.2x203.2x9.5 specimen was 19.9 which was slightly above the seismically compact slenderness limit. It was expected that this specimen would undergo more significant buckling than the previous specimens. Fig. 4(a,b) showed the onset of minor buckling in the flange during cycling to rotations of 0.04 rad. A small amount of yielding at the corner of the member was also visible. At the conclusion of the test, the buckle observed in the flange became much more pronounced (Fig. 4(c)). However, it should be noted that during the last cycle, the weld along both flanges fractured allowing the buckle to propagate downward into the rigid connection which partially affected the behavior of the member. Only minor buckling of the web near the corners of the specimen was observed. In general, minor degradation of the behavior was seen suggesting the need to further consider the extent of the width-to-thickness ratio requirements for HSS beams in seismic moment frames.

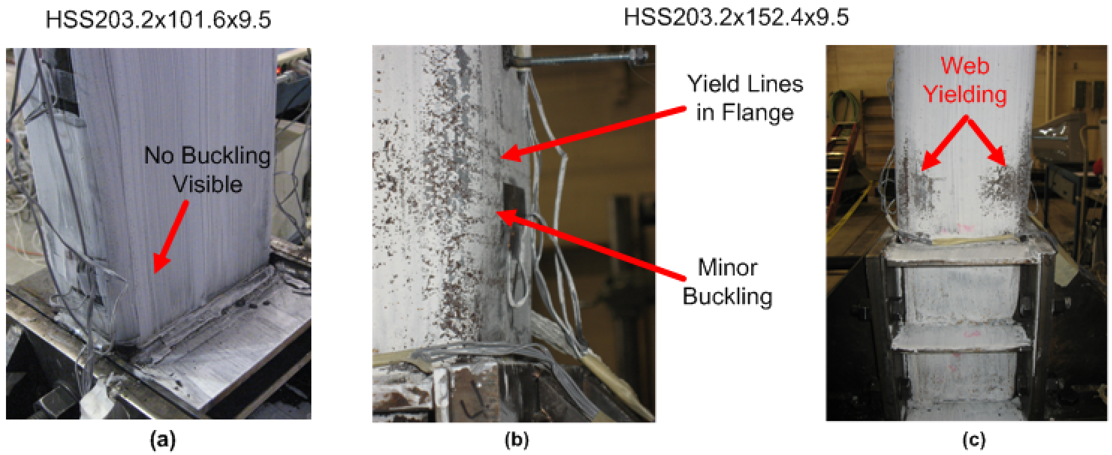

Figure 3. Photographs showing the (a) HSS203.2x101.6x9.5 specimen at the conclusion of the test and the HSS203.2x152.4x9.5 specimen (b) after cycles to 0.04 rad where buckling is first observed and (c) at the conclusion of the test.

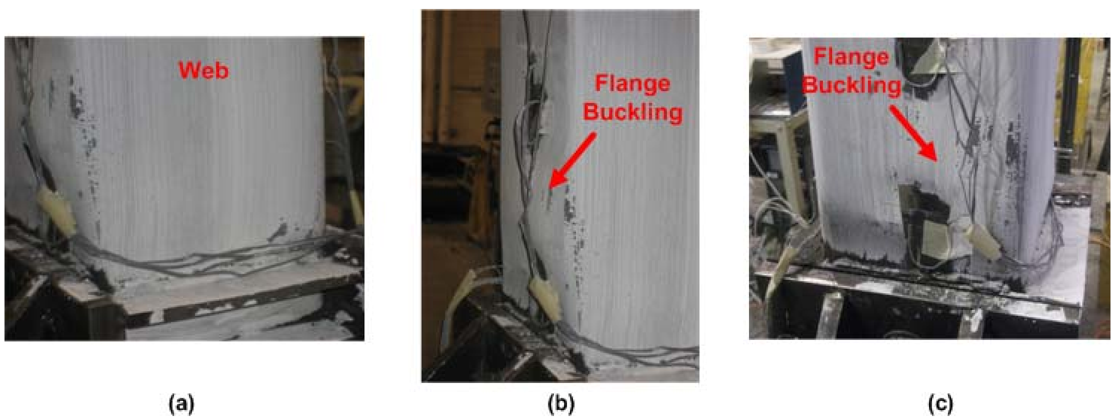

Figure 4. Photographs showing the HSS203.2x203.2x9.5 specimen (a, b) after rotations of 0.04 rad and (c) at the conclusion of the test.

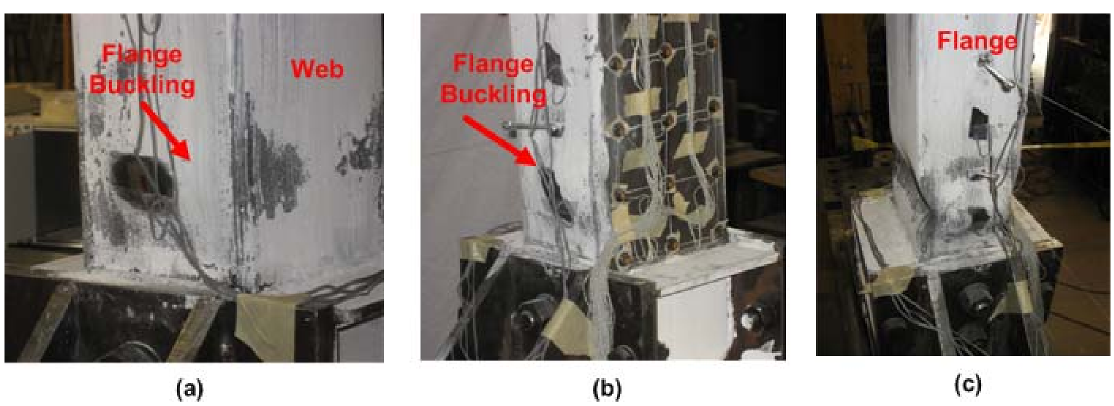

Figure 5. Photographs showing the HSS203.2x152.4x6.4 specimen (a) after rotations of 0.03 rad, (b) 0.04 rad, and (c) at the conclusion of the test.

Of the four specimens tested, the HSS203.2x152.4x6.4 (HSS8x6x1/4 in.) had the largest width-to-thickness ratio, 22.8, which resulted in significant degradation of the member behavior during cycling. Minor outward buckling of the flanges initiated during cycles to 0.03 rad (Fig.

5a). 0.03 rad was the lowest rotation level at which buckling was observed for any of the specimens. At larger rotation levels, the extent of buckling increased (Fig. 5b) until finally the web walls had buckled completely inward and the flanges showed significant outward deformation (Fig. 5c). During the later cycles, tearing of the corner material was also observed in the buckled region resulting from the cyclic tension-compression load reversal on the flanges. The depth-to-thickness ratio for the HSS203.2x152.4x6.4 specimen is also 1.5 times larger than that of the other specimens further explaining the extent of web local buckling that was observed. The behavior of this member suggested that HSS members with width-to-thickness ratios higher than 22.8 and depth-to-thickness ratios higher than 31.3 could not provide stable plastic hinging behavior necessary for use as beam members in a seismic moment frame. However, further work is still needed in order to identify the lower limit for these values.

Results

The moment-rotation curves for each of the specimen displayed a trend consistent with the previous observations where the stability of the curves was dependent on the width-to-thickness ratio. Figure 6 provides the moment-rotation curves for each specimen using the corrected rotation values accounting for the rigid body rotation and the load data obtained from the load cell.

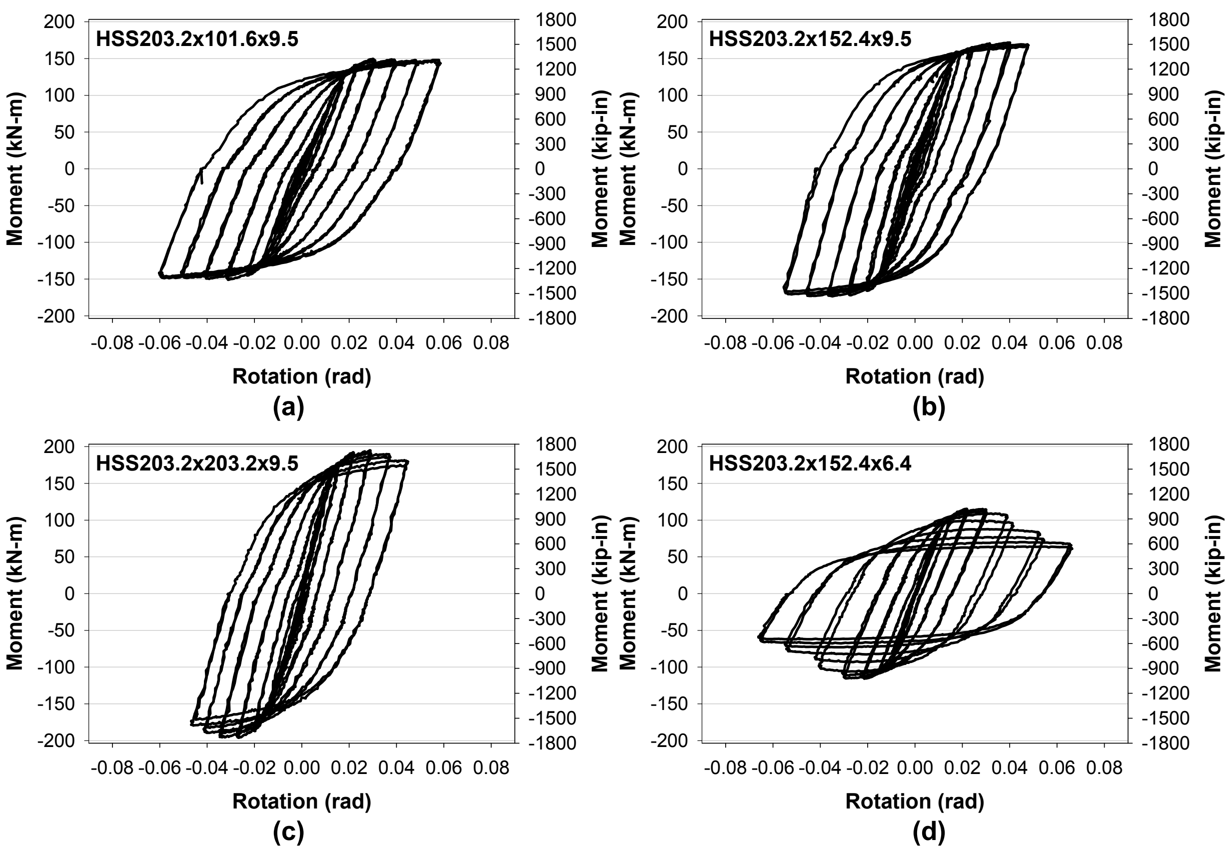

Figure 6. Moment vs. rotation curves for the (a) HSS203.2x101.6x9.5, (b) HSS203.2x152.4x9.5, (c) HSS203.2x203.2x9.5, and (d) HSS203.2x152.4x6.4 specimen.

The HSS203.2x203.2x9.5 specimen obtained the largest overall maximum moment, 196 kN-m (1733 kip-in), of the four sections tested. This could be attributed to the fact that it had the largest depth and wall thickness. Meanwhile, the HSS203.2x152.4x6.4 specimen provided the smallest overall maximum moment, 116 kN-m (1023 kip-in), as a result of a reduced wall thickness compared to the other specimens. The maximum moments reached by the other two specimens were bounded by these values and differed from each other by only 13.6 kN-m (120 kip-in).

It also was important to consider the difference between the overall maximum moment and the maximum moment measured during the final deformation cycle. This value provided a quantitative estimate of the stability of the plastic hinge behavior. Only minimal degradation of the moment capacity was observed with continued cycling of the HSS203.2x101.6x9.5 and HSS203.2x152.4x9.5 specimens. Both of these HSS beams had width-thickness ratios less than 16.1. The moment capacity for these two beams decreased by only 6.5% and 3.5%, respectively, between the overall maximum moment and the maximum moment recorded during the final loading cycle. The HSS203.2x203.2x9.5 specimen underwent a decrease in moment capacity of approximately 12% due to minor buckling of the web and flange during continued cycling. In general, all three of these specimens showed stable behavior consistent with that required of beam members in seismic moment frame systems. Meanwhile, the HSS203.2x152.4x6.4 specimen showed unacceptable levels of degradation between the overall maximum moment and the maximum moment recorded during the final cycle. The decrease in moment capacity for this member was approximately 46%. The degradation of the hysteresis behavior can easily be observed in Fig. 6(d). However, the behavior appeared to stabilize during the final set of cycles where the decrease in the moment capacity during the last two cycles appeared to mitigate. The residual rotation showed a similar trend where the HSS203.2x152.4x6.4 specimen had the largest residual rotation of 0.054 rad when cycled to zero load at the end of the test. The smallest residual rotation of all the specimens was 21% lower.

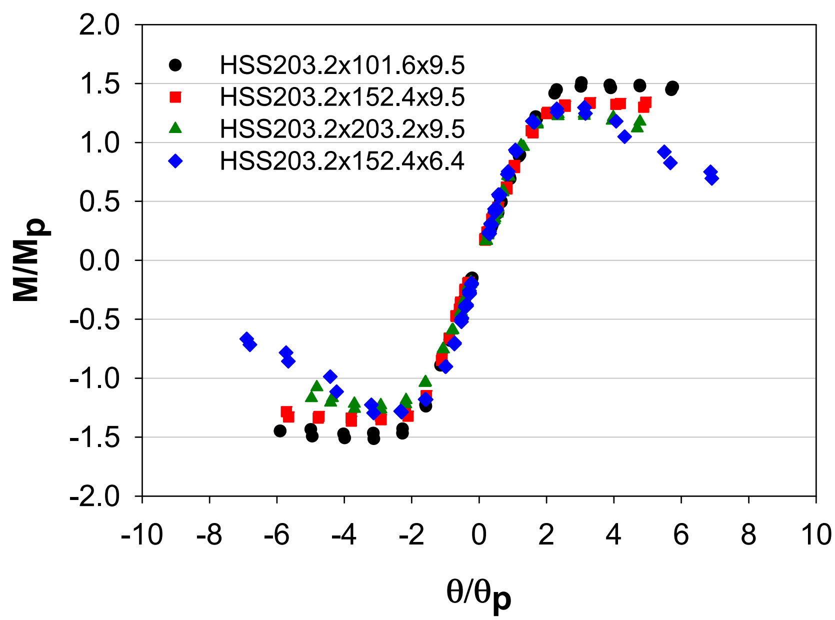

Figure 7. Normalized moment vs. rotation backbone curve for all four HSS specimens.

Figure 7 provides the backbone curves for all four specimens where the moments, *M*, measured at the maximum rotation, θ, of each loading cycle are plotted. The moment and rotation values were normalized by the theoretical plastic moment and theoretical plastic rotation, respectively. The results showed that all specimens followed a similar trend in the elastic range where the measured stiffness values are all close. Upon the onset of yielding, the plot clearly shows that both the HSS203.2x101.6x9.5 and HSS203.2x152.4x9.5 displayed only a small amount of degradation with an almost level plateau at the peak moment. Alternatively, the HSS203.2x203.2x9.5 and HSS203.2x152.4x6.4 demonstrated a clear decrease in the moment capacity after reaching their peak values. Both of these specimens also showed a decrease in maximum moment with continued cycling at a given rotation level after yielding. These results suggested the importance of the width-to-thickness ratio in the behavior of HSS beam members.

Conclusions

The cyclic inelastic behavior of four HSS beam members of varying width-to-thickness and depth-to-thickness ratios was investigated through a full-scale experimental study. The specimens were cycled to large rotation levels in order to consider their use as beam members in seismic moment frames where stable plastic hinge behavior is desired. The width-to-thickness ratio had a significant effect on the observed behavior of the specimens. When this ratio was above the seismically compact limit of 16.1 provide by AISC, flange local buckling was observed along with a degradation of the hysteresis behavior in terms of the maximum moment for a given cycle. The extent of this degradation was highly dependent on the amount in which the width-to-thickness ratio was above the seismically compact limit. The HSS203.2x203.2x9.5 had a width-to-thickness ratio of 19.9, but still showed only a minor decrease in the moment capacity of 12% which was similar to that observed for the members with width-to-thickness ratios under 16.1. This result suggested that further consideration of the limiting width-to-thickness ratio is necessary for HSS beam members under bending. However, the tests clearly demonstrated that HSS members with width-to-thickness ratios above 22.8 do not provide adequate beam behavior for seismic applications. The tests also showed that depth-to-thickness ratios of 19.1 provided adequate behavior with little to no web local buckling. Meanwhile, depth-to-thickness values above 31.1 contributed to the degradation of the plastic hinge behavior during cycling. For all of the specimens, visible local buckling did not occur until the 0.03 rad loading cycles. In general, the results suggested that adequate plastic hinge behavior can be obtained from HSS members acting as beam members, but further work is still needed to better quantify limiting width-to-thickness ratios and depth-to-thickness ratios for these sections.

Acknowledgments

The writers would like to acknowledge the help of Nadeem Banda and Jennifer Buison, undergraduate research assistants at the University of Michigan, who provided support for a portion of the experimental study. This study was supported primarily by the BRIGE Program of the National Science Foundation under Grant No. EEC-0926858.

References

American Institute of Steel Construction (AISC), 2006. *Seismic Design Manual*, American Institute of Steel Construction, Inc., Chicago, IL.

FEMA 355C, 2000. *State of the Art Report on Systems Performance of Steel Moment Frames Subject to Earthquake Ground Shaking*, SAC Joint Venture, CA.

Hajjar, J.F., 2000. Concrete-Filled Steel Tube Columns under Earthquake Loads, *Progress in Structural Engineering and Materials*, 2, 72-81.

Korol, R.M., El-Zanaty, M., Brady, F.J., 1977. Unequal Width Connections of Square Hollow Sections in Vierendeel Trusses, *Canadian Journal of Civil Engineering*, 4, 190-201.

Kumar, S.R.S. and Rao, D.V.P., 2006. RHS Beam-to-Column Connections with Web Opening-Experimental Study and Finite Element Modeling, *Journal of Constructional Steel Research*, 62, 739-746.

Kurata, M., Nakashima, M., Suita, K., 2005. Effect of Column Base Behaviour on the Seismic Response of Steel Moment Frames, *Journal of Earthquake Engineering*, 9(2), 415-438.

Kurobane, Y., 2002. Connections in Tubular Structures, *Progress in Structural Engineering and Materials*, 4, 35-45.

Nakashima, M. and Liu, D., 2005. Instability and Complete Failure of Steel Columns Subjected to Cyclic Loading, *ASCE Journal of Engineering Mechanics*, 131(6), 559-567.

Nakashima, M., Roeder, C.W., Maruoka, Y, 2000. Steel Moment Frames for Earthquakes in United States and Japan, *ASCE Journal of Structural Engineering*, 126(8), 861-868.

Nishiyama, I. and Morino, S., 2004. US-Japan Cooperative Earthquake Research Program on CFT Structures: Achievements on the Japanese Side, *Progress in Structural Engineering and Materials*, 6, 39-55.

Packer, J.A., 2000. Tubular Construction, *Progress in Structural Engineering and Materials*, 2, 41-49.

Packer, J.A. and Henderson, J.E., 1997. *Hollow Structural Section Connections and Trusses: A Design Guide*, Canadian Institute of Steel Construction, Ontario, Canada.

Rao, D.V.P. and Kumar, S.R.S., 2006. RHS Beam-to-Column Connections with Web Opening-Parametric Study and Design Guidelines, *Journal of Constructional Steel Research*, 62, 747-756.

Wang, T., McCormick, J., Yoshitake, N., Pan, P., Murata, Y., Nakashima, M., 2008. Collapse Simulation of a Four-Story Steel Moment Frame by a Distributed Online Hybrid Test, *Earthquake Engineering and Structural Dynamics*, 37, 955-974.

Wheeler, A.T., Clarke, M.J., Hancock, G.J., Murray, T.M., 1998. Design Model for Bolted Moment End Plate Connections Joining Rectangular Hollow Sections, *ASCE Journal of Structural Engineering*, 124(2), 164-173.

Wheeler, A.T., Clarke, M.J., Hancock, G.J., 2000. FE Modeling of Four-Bolt, Tubular Moment End-Plate Connections, *ASCE Journal of Structural Engineering*, 126(7), 816-822.